

Combined Differential and Common-Mode Analysis of Power Splitters and Combiners

David E. Bockelman, *Member, IEEE*, and William R. Eisenstadt, *Senior Member, IEEE*

Abstract—Power splitter/combiner phase and magnitude imbalance is analyzed in terms of simultaneous orthogonal modes of propagation. These simultaneous modes are defined as differential and common-mode. A new measure of splitter imbalance is suggested in the common-mode rejection ratio (CMRR). Measured response of 180° hybrid splitter is represented in terms of the differential and common-mode responses, and the CMRR is calculated. Combiner imbalance is also analyzed in terms of differential and common-mode responses, and response metrics are suggested. Analytical expressions for CMRR of several common splitters is given as functions of phase and magnitude imbalance.

I. INTRODUCTION

POWER SPLITTERS and combiners are indispensable components in RF and microwave systems, being used in mixers, balanced amplifiers, baluns, phase shifters, and many other applications. Some of the more commonly used splitters/combiners include 180° hybrid rings [1]–[5] and 90° branch-line couplers [6]–[8]. There are many other varieties of these components such as tightly coupled microstrip [9]–[10]. Some recent developments have focused on use of uniplanar transmission line to simplify MMIC implementations [11]–[14]. Recent MMIC applications include active splitters with an arbitrary phase relationship [15], baluns for double-balanced mixers [16], and linear vector modulators [17].

The performance of power splitters and combiners, particularly phase and magnitude balance, can have a strong influence on the performance of some systems. Systems such as a balanced *s*-parameter measurement system [18] rely on phase and magnitude relationships in power splitters/combiners to make accurate measurements. However, practical splitters/combiners, such as 3 dB hybrids, have varying amounts of phase and magnitude imbalance over their bandwidth which leads to system performance degradation or measurement errors. Typically, splitter/combiner imbalance is specified across a bandwidth in terms of maximum magnitude and phase variation [1]–[17]. Manufacturers of splitters/combiners also specify imbalance with this method. For example, a typical specification of a 1 to 12.4 GHz 180° 3 dB hybrid splitter is ± 0.8 dB amplitude imbalance and $\pm 10^\circ$ phase imbalance [19].

Manuscript received April 10, 1995; revised August 1, 1995. This work was supported in part by the Motorola Radio Products Group Applied Research.

D. E. Bockelman is with Motorola Radio Products Applied Research, Plantation, FL 33322 USA.

W. R. Eisenstadt is with the University of Florida, Gainesville, FL 32611 USA.

IEEE Log Number 9414849.

This paper presents an analysis of imbalances in power splitters and combiners in terms of differential and common-modes. The analysis yields approximate expressions for the differential and common-mode normalized waves as a function of magnitude and phase imbalance. These expressions demonstrate that splitter/combiner imbalance can be represented in terms of differential and common-mode responses, and provide insight into the nature of such responses. The combined differential and common-mode analysis represents a more complete way of quantifying imbalance, and new performance metrics are suggested to simultaneously characterize phase and magnitude imbalance. These metrics promote a fundamental understanding of the physical performance of nonideal splitters and combiners which is useful in the design and analysis of sensitive differential circuits and systems.

II. DEFINITIONS

Consider a splitter, such as a hybrid splitter, which has a single input and two outputs. The relationships between the two outputs can be described in several ways, but we choose to represent the total voltages and currents at the outputs in terms of differential and common-mode voltages and currents. The definitions of these quantities for a two output system are reported in the literature [20], and are repeated below

$$v_{dm} \equiv v_1 - v_2 \quad (1)$$

$$i_{dm} \equiv \frac{1}{2}(i_1 - i_2) \quad (2)$$

$$v_{cm} \equiv \frac{1}{2}(v_1 + v_2) \quad (3)$$

$$i_{cm} \equiv i_1 - i_2 \quad (4)$$

where v_1 and v_2 are the voltages at outputs 1 and 2, respectively, and i_1 and i_2 are the currents flowing into outputs 1 and 2, respectively. From these voltages and currents, it has been shown that the differential and common-mode normalized waves can be expressed as [20]

$$b_{dm} = \frac{1}{\sqrt{2}}(b_1 - b_2) \quad (5)$$

$$b_{cm} = \frac{1}{\sqrt{2}}(b_1 + b_2) \quad (6)$$

where b_1 and b_2 are normalized output waves at ports 1 and 2, respectively.

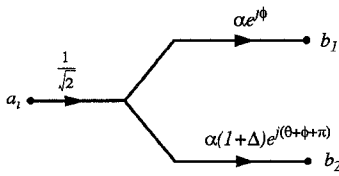


Fig. 1. Simplified signal flowgraph of 180° 3 dB splitter with phase and amplitude imbalance.

III. DIFFERENTIAL AND COMMON-MODE WAVES IN 180° SPLITTER

To continue the analysis, we will choose a specific type of splitter/combiner, say a 180° 3 dB hybrid used in a splitter configuration. A simplified signal flow graph of this device is shown in Fig. 1, neglecting port mismatch and the output-to-output signal path. Included in this flow graph is the amplitude imbalance (Δ), phase imbalance (θ), balanced loss (α), and balanced phase shift (ϕ). Note, the outputs of the splitter are ideally of equal magnitude and 180° out of phase.

From (5) and Fig. 1, the differential-mode normalized output can be found to be

$$b_{dm} = \frac{\alpha a_i e^{j\phi}}{2} (1 + (1 + \Delta) e^{j\theta}) \quad (7)$$

where a_i is the normalized input wave. Similarly, from (6) the common-mode normalized output can be found to be

$$b_{cm} = \frac{\alpha a_i e^{j\phi}}{2} (1 - (1 + \Delta) e^{j\theta}). \quad (8)$$

If the phase imbalance is small ($|\theta| \ll 1$) then the complex exponential can be approximated by

$$e^{j\theta} \approx 1 + j\theta. \quad (9)$$

Applying this approximation to (7), the differential-mode normalized output can be approximated as

$$b_{dm} \approx \frac{\alpha a_i e^{j\phi}}{2} (2 + \Delta + j\theta(1 + \Delta)) \quad (10)$$

which can be expressed as

$$b_{dm} \approx \frac{\alpha a_i e^{j\phi}}{2} \sqrt{(2 + \Delta)^2 + \theta^2(1 + \Delta)^2} \times \exp\left(j \arctan\left(\frac{\theta(1 + \Delta)}{2 + \Delta}\right)\right) \quad (11)$$

which can be further approximated by

$$b_{dm} \approx \frac{\alpha a_i e^{j\phi}}{2} \sqrt{(2 + \Delta)^2 + \theta^2(1 + \Delta)^2} e^{j\theta\left(\frac{1+\Delta}{2+\Delta}\right)} \approx \frac{\alpha a_i e^{j\phi}}{2} (2 + \Delta) e^{j(\theta/2)} \quad (12)$$

where the final approximation assumes the imbalances to be small ($|\theta| \ll 1, \Delta \ll 1$). In a similar fashion, the common-

mode normalized output wave (8) from the splitter can be approximated by

$$\begin{aligned} b_{cm} &\approx \frac{-\alpha a_i e^{j\phi}}{2} \sqrt{\Delta^2 + \theta^2(1 + \Delta)^2} e^{j\left(\frac{\theta(1+\Delta)}{\Delta}\right)} \\ &\approx \frac{-\alpha a_i e^{j\phi}}{2} \sqrt{\Delta^2 + \theta^2} e^{j(\theta/\Delta)}. \end{aligned} \quad (13)$$

In the case of a 180° splitter, the common-mode wave can be considered to be an unintended signal, and its magnitude is directly proportional to magnitude imbalance of the splitter. The phase imbalance has a second order effect on the magnitude of the common-mode wave, but it has a more significant effect on the phase of the common-mode signal. As can be seen from (12), the magnitude of the differential-mode wave is effected primarily by the magnitude imbalance of the splitter. However, since $\Delta \ll 1$, we can see the splitter imbalance is a small error in the desired output signal.

The common-mode rejection ratio can be adapted from differential circuit concepts as a measure of the imbalance in a splitter. The common-mode rejection ratio (CMRR) [21] can be adapted to normalized waves by the definition

$$\text{CMRR} \equiv \left| \frac{b_{dm}}{b_{cm}} \right| \quad (14)$$

which, in the case of a 180° splitter, can be approximated by

$$\text{CMRR} \approx \sqrt{\frac{(2 + \Delta)^2 + \theta^2(1 + \Delta)^2}{\Delta^2 + \theta^2(1 + \Delta)^2}} \approx \frac{2 + \Delta}{\sqrt{\Delta^2 + \theta^2}}. \quad (15)$$

This quantity gives a single measure of the effects of both magnitude and phase imbalance in a splitter.

The relation between CMRR and the traditional measures of imbalance can be examined by plotting contours of constant CMRR from (14) as a function of θ and $1 + \Delta$, as shown in Fig. 2. By plotting θ and $1 + \Delta$ in rectangular coordinates, these contours form ellipses, and by choosing units of degrees and dB for phase and magnitude imbalance, respectively, the specifications can be plotted on the same plane as horizontal and vertical lines. The phase and magnitude imbalance specification lines define a rectangle in the imbalance plane. The lowest CMRR in this rectangle, the result of maximum phase and maximum magnitude imbalance occurring simultaneously, is indicated by the ellipse which intersects the corners of the rectangle.

Another significant ellipse is the one which is entirely contained in the specification rectangle. This ellipse represents the highest CMRR that can occur while one of the imbalances is at its maximum specified limit. In Fig. 2, such an ellipse is limited by the magnitude imbalance, indicating the worst-case best performance is limited by magnitude imbalance. The shaded regions in Fig. 2 indicate performance that is within the traditional specification limits, but has relatively poor CMRR.

Had the phase specifications been made such that their representative lines were also tangent to the smallest dashed

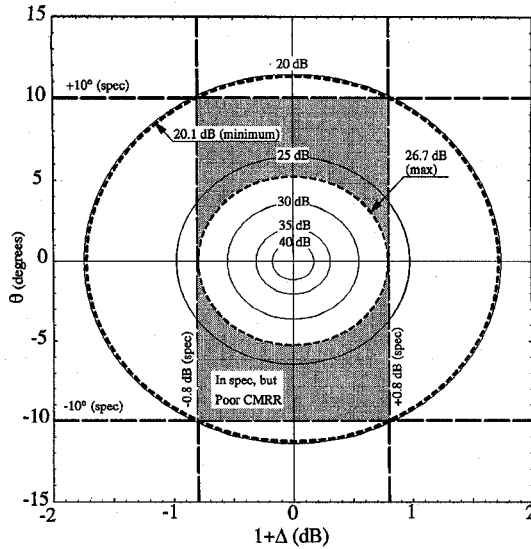


Fig. 2. Loci of constant CMRR (dB) in the plane of phase imbalance, θ (degrees), versus magnitude imbalance, $1 + \Delta$ (dB). Dashed lines indicate manufacturer's specifications, and dashed ellipses indicate worst-case and best-case CMRR interpretation of specifications. Shaded regions indicate performance within specification with poor CMRR.

ellipse, areas of lower CMRR would still exist in the corners of the resulting rectangle. These regions illustrate the advantage of specifying minimum CMRR over maximum magnitude and phase imbalance. Two splitters with the same magnitude and phase specifications may have different minimum CMRR. However, if minimum CMRR is specified, no such ambiguity exists, and the CMRR ellipse indicates the maximum simultaneous phase and magnitude imbalance.

IV. MEASURED SPLITTER RESULTS

To illustrate the use of above analysis, the s-parameters of a 180° 3 dB hybrid splitter/combiner (Merrimac, part number HJM-4R-6.5G) were measured. The measurements were made on a Hewlett-Packard 8510C vector network analyzer (VNA) with 3.5 mm coaxial connectors, with a sliding-load TOSL calibration. As the VNA is a two-port analyzer, the remaining ports of the splitter were terminated with precision 50Ω loads. A total of three two-port s-parameter sets were generated as the three ports were measured two at a time, with the remaining port terminated. The errors due to any imperfect termination of the free port were considered to be negligibly small. The overall three-port s-parameters of the splitter were constructed from the appropriate elements of the three two-port s-parameter sets.

A direct measurement of the output magnitude imbalance is shown in Fig. 3(a). This power splitter is specified to have no more than ± 0.8 dB magnitude variation from 1 to 12.4 GHz. The measured phase imbalance is shown in Fig. 3(b). Over its bandwidth, this splitter should have a maximum phase variation of $\pm 10^\circ$. As can be seen from these figures, the splitter is within specification.

The differential and common-mode response of the splitter was calculated from the measured s-parameters. With the definitions $S_{1i} = b_1/a_i$, and $S_{2i} = b_2/a_i$, and the use of

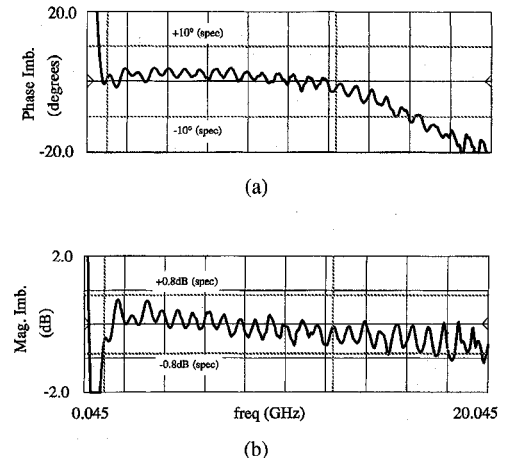


Fig. 3. (a) Measured magnitude imbalance in dB of a 180° 3 dB hybrid power splitter with dashed lines indicating manufacturer's specifications. (b) Measured phase imbalance in degrees of same 180° 3 dB hybrid power splitter with dashed lines indicating manufacturer's specifications.

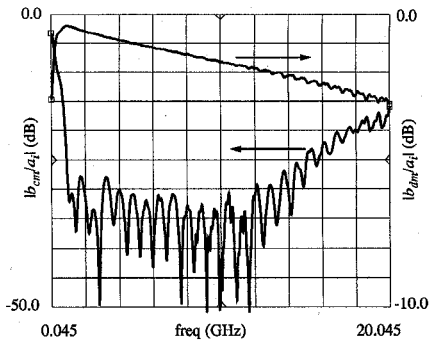


Fig. 4. Ratio in dB of normalized common-mode-to-input waves and normalized differential-mode-to-input waves of a 180° 3 dB hybrid power splitter. Data is derived from measured data. Note the different vertical scales.

(5) and (6), it is easily shown that

$$\begin{aligned} S_{dm} &\equiv \frac{b_{dm}}{a_i} = \frac{1}{\sqrt{2}}(S_{1i} - S_{2i}) \\ S_{cm} &\equiv \frac{b_{cm}}{a_i} = \frac{1}{\sqrt{2}}(S_{1i} + S_{2i}) \end{aligned} \quad (16)$$

which are readily calculated from measured data. The magnitude of these differential and common-mode s-parameters are shown in Fig. 4. This figure clearly shows the generation of a common-mode signal at the output of the splitter. Outside of the splitter's intended bandwidth, the common-mode response becomes large in magnitude, and the differential-mode response shows ripple in its magnitude.

The CMRR of the splitter can also be easily calculated from measured s-parameters. With the use of (14) and (16)

$$CMRR = \left| \frac{S_{dm}}{S_{cm}} \right| = \left| \frac{S_{1i} - S_{2i}}{S_{1i} + S_{2i}} \right|. \quad (17)$$

The calculated CMRR magnitude is shown in Fig. 5. In the specified bandwidth, the splitter has approximately 30 dB CMRR, decreasing rapidly out of band. The minimum measured CMRR is 27.2 dB.

The measured imbalance is plotted on the imbalance plane of θ and $1 + \Delta$ in Fig. 6 over the specification bandwidth of

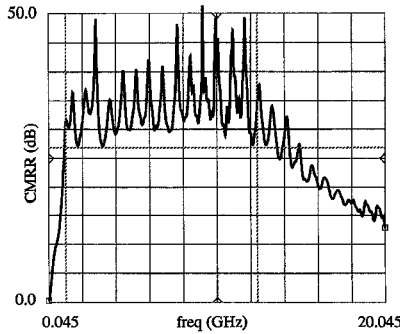


Fig. 5. Common-mode rejection ratio (magnitude) in dB of a 180° 3 dB hybrid power splitter. Data is derived from measured data.

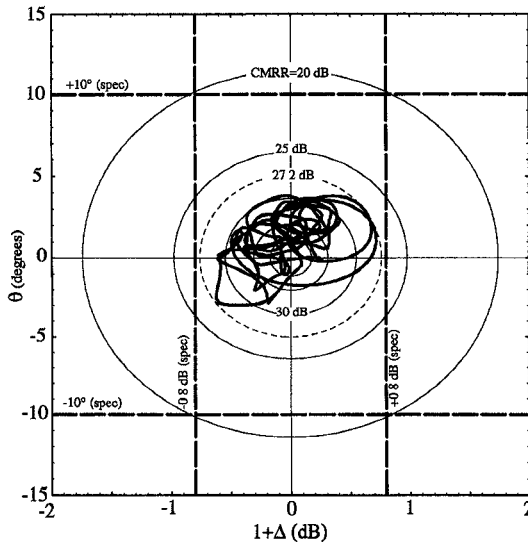


Fig. 6. Measured imbalance of 180° 3 dB hybrid power splitter (1.0 GHz to 12.4 GHz) plotted in the plane of phase imbalance, θ (degrees), versus magnitude imbalance, $1 + \Delta$ (dB), with loci of constant CMRR (dB). Dashed lines indicate manufacturer's specifications, and dashed ellipse indicates minimum measured CMRR.

1.0 GHz to 12.4 GHz. The data is entirely contained within the 27.2 dB ellipse, which falls within the limits of the highest possible CMRR specification of 26.7 dB (Fig. 2).

V. COMBINERS

The effect of magnitude and phase imbalance on power combiners can also be analyzed in terms of differential and common-mode normalized waves. In a typical hybrid power splitter/combiner, two signals will be combined in two fashions simultaneously, producing two outputs. For example, the 3 dB hybrid 180° splitter/combiner will produce the sum of two input signals at one output and the difference of the signals at the second output. The combiner can be analyzed as two single output combiners, each delivering the sum or difference signal as appropriate. Therefore, we will consider only a 180° combiner, with generalizations to any phase of combining. The simplified signal flow graph of a 180° combiner is similar to that of the splitter, and is shown in Fig. 7. At each input, there is assumed to be a linear combination of differential and

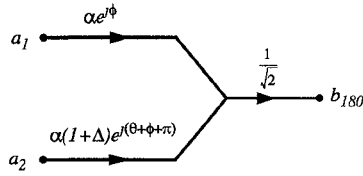


Fig. 7. Simplified signal flowgraph of 180° 3 dB combiner with phase and amplitude imbalance.

common-mode waves

$$a_1 = \frac{a_{cm} + a_{dm}}{\sqrt{2}} \quad a_2 = \frac{a_{cm} - a_{dm}}{\sqrt{2}} \quad (18)$$

which can be found by solving the forward wave relations similar to (5) and (6) for a_1 and a_2 . The total output of the combiner is then a function of a_{dm} , a_{cm} and imbalances Δ and θ . The 180° combiner has an output

$$b_{180} = \frac{\alpha e^{j\phi}}{2} [(a_{cm} + a_{dm}) - (1 + \Delta) e^{j\theta} (a_{cm} - a_{dm})]. \quad (19)$$

A rejection ratio can not be directly applied to combiners. However, a common-mode combiner response ratio (RCM_{comb}) can be defined as

$$RCM_{comb} \equiv \left| \frac{b_{180}}{a_{cm}} \right|_{a_{dm}=0} \quad (20)$$

which can be shown to be approximately

$$RCM_{comb} \approx \frac{\alpha}{2} \sqrt{\Delta^2 + \theta^2 (1 + \Delta)^2}. \quad (21)$$

Equations (19) and (21) indicate that, due to imbalance, the output of the combiner is clearly influenced by the presence of a common-mode signal at the inputs.

In addition to a response from an undesired mode, imbalance in the combiner also causes error in the combining of the desired mode. To illustrate this, consider the differential-mode response ratio (RDM_{comb}) of the 180° combiner defined as

$$RDM_{comb} \equiv \left| \frac{b_{180}}{a_{dm}} \right|_{a_{cm}=0} \approx \frac{\alpha}{2} \sqrt{(2 + \Delta)^2 + \theta^2 (1 + \Delta)^2}. \quad (22)$$

This illustrates the error in the combination of the desired mode is a function of imbalance. It is interesting to note that the ratio of (22) and (21) is equal to the CMRR of the splitter in (15).

The measured s -parameters of the example splitter of Section IV can also be examined for combiner performance. The response ratios of (20) can be related to the measured s -parameters by

$$RCM_{comb} = \left| \frac{b_3}{(a_1 + a_2)/\sqrt{2}} \right| = \sqrt{2} \left| \frac{a_1}{b_3} + \frac{a_2}{b_3} \right|^{-1} \\ = \sqrt{2} \left| \frac{1}{S_{31}} + \frac{1}{S_{32}} \right|^{-1} \quad (23)$$

where port 3 is the output and ports 1 and 2 are the inputs. Similarly, the response ratios of (22) can be related to the measured s -parameters by

$$RDM_{comb} = \sqrt{2} \left(\frac{1}{S_{31}} - \frac{1}{S_{32}} \right)^{-1}. \quad (24)$$

TABLE I
SPLITTER CMRR FOR COMMON VALUES OF Ω

| Ω | CMRR (1 st approx.) | CMRR (2 nd approx.) | Ideal Value |
|----------|--|--|-------------|
| 0° | $\frac{\Delta^2 + \theta^2 (1 + \Delta)^2}{\sqrt{(2 + \Delta)^2 + \theta^2 (1 + \Delta)^2}}$ | $\frac{\sqrt{\Delta^2 + \theta^2}}{2 + \Delta}$ | 0 |
| 90° | $\frac{(1 + \theta (1 + \Delta))^2 + (1 + \Delta)^2}{\sqrt{(1 - \theta (1 + \Delta))^2 + (1 + \Delta)^2}}$ | $\frac{1 + \Delta + \theta}{\sqrt{1 + \Delta - \theta}}$ | 1 |
| 180° | $\frac{(2 + \Delta)^2 + \theta^2 (1 + \Delta)^2}{\sqrt{\Delta^2 + \theta^2 (1 + \Delta)^2}}$ | $\frac{2 + \Delta}{\sqrt{\Delta^2 + \theta^2}}$ | ∞ |

Plots of these ratios are not included in this paper since they are closely related the splitter performance shown in Fig. 5.

VI. EXTENSIONS TO ARBITRARY PHASE

The above combined differential and common-mode analysis suggests an alternate, and useful, way of interpreting the imbalances in a splitter/combiner. The measured s -parameters of a practical power splitter further illustrate the combined-mode, or mixed-mode, concepts. From the application of these concepts, CMRR is found to quantify the effects of both magnitude and phase imbalance in power splitters. The above analysis considers only a 180° power splitter, but the analysis is easily extended to an arbitrary phase relation. For an arbitrary phase splitting the CMRR is exactly

$$\text{CMRR} = \left| \frac{1 - (1 + \Delta)e^{j(\Omega + \theta)}}{1 + (1 + \Delta)e^{j(\Omega + \theta)}} \right| \quad (25)$$

where Ω is the phase of the split (e.g. 0°, 180°). With first order approximations, (25) has been simplified for three common angles, and these results are summarized in Table I. A study of errors resulting from the approximations ($|\theta| \ll 1, \Delta \ll 1$) indicates both forms to be quite accurate over practical values of phase and magnitude imbalance. For a CMRR of 25 dB, both approximations have a maximum error of less than ± 0.2 dB. Note that when Ω is not 180°, CMRR does not have the traditional meaning or value, so that its name is misleading. For example, with $\Omega = 0^\circ$ CMRR is ideally zero since the differential-mode output is ideally zero. For 0° splitters/combiners another metric is more conceptually natural, namely differential-mode-rejection (DMRR) which can be defined as $\text{DMRR} = 1/\text{CMRR}$. For 90°, and other angles, neither DMRR nor CMRR is interpreted in a typical fashion. The use of the single metric CMRR for all phases of splitters is both simple and accurate, if its meaning is properly interpreted for each phase splitter.

The effects of magnitude and phase imbalance in power combiners have also been described through a mixed-mode analysis. Response ratios such as RDM and RCM quantify these effects. The combiner analysis considers only a 180° power combiner, but the analysis is easily extended to an arbitrary phase relation. For an arbitrary phase combining these

TABLE II
COMBINER RDM AND RCM FOR COMMON VALUES OF Ω

| Ω | RDM | RCM |
|----------|--|--|
| 0° | $\frac{\alpha}{2} \sqrt{\Delta^2 + \theta^2 (1 + \Delta)^2}$ | $\frac{\alpha}{2} \sqrt{(2 + \Delta)^2 + \theta^2 (1 + \Delta)^2}$ |
| 90° | $\frac{\alpha}{2} \sqrt{(1 + \theta (1 + \Delta))^2 + (1 + \Delta)^2}$ | $\frac{\alpha}{2} \sqrt{(1 - \theta (1 + \Delta))^2 + (1 + \Delta)^2}$ |
| 180° | $\frac{\alpha}{2} \sqrt{(2 + \Delta)^2 + \theta^2 (1 + \Delta)^2}$ | $\frac{\alpha}{2} \sqrt{\Delta^2 + \theta^2 (1 + \Delta)^2}$ |

responses are exactly

$$\begin{aligned} \text{RDM} &= \frac{\alpha}{2} \left| 1 - (1 + \Delta)e^{j(\Omega + \theta)} \right| \\ \text{RCM} &= \frac{\alpha}{2} \left| 1 + (1 + \Delta)e^{j(\Omega + \theta)} \right|. \end{aligned} \quad (26)$$

To a first order approximation, (26) has been simplified for three common angles, and these results are summarized in Table II.

VII. CONCLUSION

The impact on systems using power splitters and combiners can now be considered in terms of differential and common-mode responses. The effects of an undesired signal mode, such as common-mode, can be investigated with simple network theory, and limits on such undesired signals can be set through the use of CMRR.

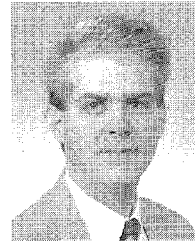
ACKNOWLEDGMENT

D. E. Bockelman would like to thank C. Backof and W.-Y. Howng for their support during the pursuit of his degree.

REFERENCES

- [1] C. H. Ho, L. Fan, and K. Chang, "Ultra wide band slotline hybrid-ring couplers," in *IEEE Microwave Theory Tech.-S Int. Microwave Symp. Dig.*, 1992, pp. 1175-1178.
- [2] G. F. Mikucki and A. K. Agrawal, "A broad-band printed circuit hybrid-ring power divider," *IEEE Trans. Microwave Theory Tech.*, vol. 37, pp. 112-117, Nov. 1989.
- [3] D. Kim and Y. Naito, "Broad-band design of improved hybrid-ring 3 dB directional coupler," *IEEE Trans. Microwave Theory Tech.*, vol. MTT-30, pp. 2040-2046, Nov. 1982.
- [4] C. Y. Pon, "Hybrid-ring directional couplers for arbitrary power division," *IRE Trans. Microwave Theory Tech.*, vol. MTT-9, pp. 529-535, Nov. 1961.
- [5] E. M. T. Jones, "Wide-band strip-line magic-T," *IRE Trans. Microwave Theory Tech.*, vol. MTT-8, pp. 160-168, Mar. 1960.
- [6] M. Muraguchi, T. Yukitake, and Y. Naito, "Optimum design of 3-dB branch-line couplers using microstrip lines," *IEEE Trans. Microwave Theory Tech.*, vol. MTT-31, pp. 674-678, Aug. 1983.
- [7] R. Levy and L. Lind, "Synthesis of symmetrical branch-guide directional couplers," *IEEE Trans. Microwave Theory Tech.*, vol. MTT-16, pp. 80-89, Feb. 1968.
- [8] L. Young, "Branch guide directional couplers," in *Proc. Nat. Electron. Conf.*, 1956, vol. 12, pp. 723-732.
- [9] D. Willems and I. Bahl, "An MMIC-Compatible tightly coupled line structure using embedded microstrip," *IEEE Trans. Microwave Theory Tech.*, vol. 41, pp. 2303-2310, Dec. 1993.
- [10] S. Arai, A. Kato, K. Minami, and T. Nishikawa, "A 900MHz 90 degrees hybrid for QPSK modulator," in *IEEE Microwave Theory Tech.-S Int. Microwave Symp. Dig.*, 1991, pp. 857-860.

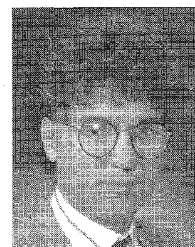
- [11] C. H. Ho, L. Fan, and K. Chang, "Broad-band uniplanar hybrid-ring and branch-line couplers," *IEEE Trans. Microwave Theory Tech.*, vol. 41, pp. 2116-2124, Dec. 1993.
- [12] T. Hirta, Y. Tarusawa, and H. Ogawa, "Uniplanar MMIC hybrids—A proposed new MMIC structure," *IEEE Trans. Microwave Theory Tech.*, vol. MTT-35, pp. 576-581, June 1987.
- [13] J. A. Navarro, Y. H. Shu, and K. Chang, "Broad-band electronically tunable planar active radiating elements and spatial power combiners using notch antennas," *IEEE Trans. Microwave Theory Tech.*, vol. 40, pp. 323-328, Feb. 1992.
- [14] T. Tokumitsu, S. Hara, and M. Aikawa, "Very small ultra-wideband MMIC magic-T and applications to combiners and dividers," *IEEE Trans. Microwave Theory Tech.*, vol. 37, pp. 1985-1990, Dec. 1989.
- [15] H. Kamitsuna and H. Ogawa, "Ultra-wideband MMIC active power splitters with arbitrary phase relationships," *IEEE Trans. Microwave Theory Tech.*, vol. 41, pp. 1519-1523, Sept. 1993.
- [16] T. H. Chen *et al.*, "Broadband monolithic passive baluns and monolithic double-balanced mixer," in *IEEE Microwave Theory Tech. MTT-S Int. Microwave Symp. Dig.*, 1991, pp. 861-864.
- [17] F. L. M. van den Bogart and R. Pyndiah, "A 10-14 GHz linear MMIC vector modulator with less than 0.1 dB and 0.8 amplitude and phase error," in *IEEE Microwave Theory Tech. MTT-S Int. Microwave Symp. Dig.*, 1990, pp. 465-468.
- [18] Application Note: WPH-505/805 Waveguide-Input Wafer Probes, Cascade Microtech, Beaverton, OR, 1993.
- [19] Product Data Pack: HJM-4R-6.5G 180 Power Divider/Combiner, Merrimac Industries, West Caldwell, NJ, June 1993.
- [20] D. E. Bockelman and W. R. Eisenstadt, "Combined differential and common mode scattering parameters: Theory and simulation," *IEEE Trans. Microwave Theory Tech.*, vol. 43, no. 7, pp. 1530-1539, July 1995.
- [21] P. R. Gray and R. G. Meyer, *Analysis and Design of Analog Integrated Circuits*, 3rd. ed. New York: Wiley, 1993.



David E. Bockelman (S'88-M'90) received the B.S. and M.S. degrees in electrical engineering from the Georgia Institute of Technology, Atlanta, GA, in 1989 and 1990, respectively. He is currently is pursuing the Ph.D. degree in electrical engineering at the University of Florida, Gainesville, FL.

He joined the Applied Research Department of Motorola Radio Products Group in 1990, where he is currently a Senior Engineer. His work has included microwave device characterization and modeling, and active device noise measurement. His current interests include distortion theory, nonlinear modeling, and microwave circuit design. He holds five patents.

Mr. Bockelman is a member of Eta Kappa Nu and is a registered Professional Engineer.



William R. Eisenstadt (S'78-M'84-SM'92) received the B.S., M.S., and Ph.D. degrees in electrical engineering from Stanford University, Stanford, CA, in 1979, 1981, and 1986, respectively.

In 1984, he joined the faculty of the University of Florida, Gainesville, FL, where he is now an Associate Professor. His research is concerned with high-frequency characterization, simulation and modeling of integrated circuit devices, packages, and interconnect. In addition, he is interested in large-signal microwave circuit and analog circuit design.

Dr. Eisenstadt received the NSF Presidential Young Investigator Award in 1985.